Carbohydrate Polymers 115 (2015) 207–214

Contents lists available at ScienceDirect

Carbohydrate Polymers

journal homepage: www.elsevier.com/locate/carbpol

Changes of wood cell walls in response to hygro-mechanical steam treatment

Juan Guo[a,1], Kunlin Song[a,1], Lennart Salmén[b,c,*], Yafang Yin[a,b,*]

[a] Department of Wood Anatomy and Utilization, Research Institute of Wood Industry, Chinese Academy of Forestry, Beijing 100091, China
[b] Wallenberg Wood Science Center, Royal Institute of Technology (KTH), Stockholm SE-10044, Sweden
[c] Innventia AB, Box 5604, Stockholm, SE-11486, Sweden

ARTICLE INFO

Article history:
Received 1 April 2014
Received in revised form 6 August 2014
Accepted 9 August 2014
Available online 27 August 2014

Keywords:
Cell wall
Hygro-mechanical steam treatment
Earlywood
Latewood
Biopolymer components

ABSTRACT

The effects of compression combined with steam treatment (CS-treatment), i.e. a hygro-mechanical steam treatment on Spruce wood were studied on a cell-structure level to understand the chemical and physical changes of the secondary cell wall occurring under such conditions. Specially, imaging FT-IR microscopy, nanoindentation and dynamic vapour absorption were used to track changes in the chemical structure, in micromechanical and hygroscopic properties. It was shown that CS-treatment resulted in different changes in morphological, chemical and physical properties of the cell wall, in comparison with those under pure steam treatment. After CS-treatment, the cellular structure displayed significant deformations, and the biopolymer components, e.g. hemicellulose and lignin, were degraded, resulting in decreased hygroscopicity and increased mechanical properties of the wood compared to both untreated and steam treated wood. Moreover, CS-treatment resulted in a higher degree of degradation especially in earlywood compared to a more uniform behaviour of wood treated only by steam.

1. Introduction

Wood is one of the oldest composite structures man has made use of, in which thousands of primary structure building blocks of tracheids or fibres packed orderly together. In softwoods, about 94% of the wood cells are tracheids (Havimo et al., 2007). Earlywood tracheids, with a thinner wall and wider lumen, and latewood tracheids, with a much thicker wall and narrow lumen, can be observed in an integrated growth ring (Richter et al., 2004; Panshin & Zeeuw, 1970). The wood cell wall is even more structurally advanced, whose structure is principally composed of cellulose microfibrils embedded in a matrix composed of lignin and hemicelluloses (Fengel & Wegener, 1984).

As a renewable resource with an exceptional strength-to-weight ratio, the utilization of wood is restricted by the lack of dimensional stability, low resistance to decay, and poor durability (Hill, 2006). Thus there has recently been a renewed interest in wood modification. Among the various techniques for improving the quality of wood, wood densification (Kollmann et al., 1975; Inoue et al., 1990; Kutnar & Šernek, 2007; Homan & Jorissen, 2004) has been thought to be a promising method, aiming to acquire desired functionality without changing the advantages of wood. Densification undoubtedly improves certain mechanical and physical properties of wood but the transformed shape (compression deformation) produced during densification is unstable and is easy recovered totally or partially after re-moistening and heating.

Until now, large efforts in chemical modification (Ermeydan et al., 2012; Trey et al., 2010; Ermeydan et al., 2014; Deka & Saikia, 2000; Jebrane et al., 2011; Yuan et al., 2013; Jebrane & Sèbe, 2008) have been devoted to maintain permanent fixation of wood materials. Hydro-thermal treatment (Esteves & Pereira, 2009; Todaro et al., 2012; Lam et al., 2013; Tooyserkani et al., 2013) and thermo-hygro-mechanical treatment (Navi & Girardet, 2005; Welzbacher et al., 2008; Diouf et al., 2011; Cai et al., 2013) remain challenging and attractive since they are efficient and ecofriendly strategies to improve the dimensional stability and durability of wood.

However, the influence and mechanisms of the steam degradation process and rearrangement of biomolecules under compressive condition, with regard to changes in the chemical structure and in the mechanical properties on a cellular level, have not been fully characterized and understood. In a previous paper

* Corresponding authors at: Innventia AB, Box 5604, Stockholm, SE-11486, Sweden; Chinese Academy of Forestry, Department of Wood Anatomy and Utilization, Research Institute of Wood Industry, No. 1 Dongxiaofu, Beijing 100091, China. Tel.: +86 62889468/+46 8 6767340; fax: +86 62881937/+46 8 4115518.
E-mail addresses: lennart.salmen@innventia.com (L. Salmén), yingyafangcaf@gmail.com, yafang@caf.ac.cn (Y. Yin).
[1] These authors contributed equally.

http://dx.doi.org/10.1016/j.carbpol.2014.08.040
0144-8617/

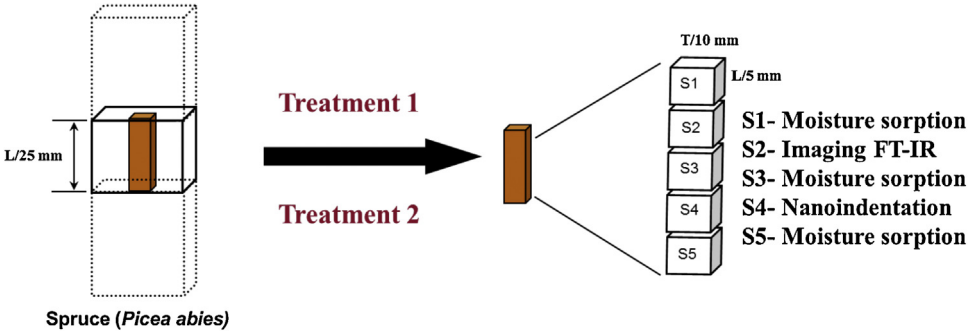

Fig. 1. Scheme of preparation of wood samples for Imaging FT-IR, moisture sorption, and nanoindentation measurements. Treatment 1: the CS-treatment; Treatment 2: high-temperature steam treatment.

(Yin et al., 2011), we reported effects of high-temperature steam treatment on the chemical and physical changes of softwood on a cell-structure level. It was indicated that chemical changes in the biopolymer components of the cell wall could fully account for the changes observed in the hygroscopicity and indentation modulus of the wood material while no major difference was detected between the effects of the steam treatment on earlywood and latewood.

In this paper, the effects of compression together with a hygrothermal treatment were studied on the chemical and physical changes of Spruce (*Picea abies* Karst.) on a cell-structure level (the term "hygro" refers to treatments using water steam (e.g. high pressure steam) as compared to the term "hydro" which is used to describe treatments using water). Specifically, imaging FT-IR microscopy was utilized to track the variations in chemical structures under compression combined with steam treatment (CS-treatment) on a micrometer level. Moreover, nanoindentation, a method of mechanical testing on a submicrometer scale that highlights structural variations in biomaterials, such as wood and bamboo (Ermeydan et al., 2012; Vincent et al., 2014; Gindl et al., 2004; Gershon et al., 2010; Yu et al., 2007; Oliver & Pharr, 1992) was used. Furthermore, the influences on the earlywood and latewood structures were explored. The results would promote the understanding of the effect and mechanism of steam degradation and rearrangement of biomolecules under compressed condition and also provide a scientific basis for the development of environmentally friendly wood products that may have the potential to substitute the wide use of chemical preservatives for wood.

2. Materials and methods

2.1. Materials

Small specimens (dimensions 20 × 20 × 25 mm in the tangential (T), radial (R), and longitudinal (L) directions, respectively) cut from Spruce (*Picea abies* Karst.) wood lumber were treated by CS-treatment. The CS-treatment was conducted with a 50% radial compression ratio (the percentage of the decrease in thickness to the initial thickness of the specimen) at 110 °C for 6 minutes (min) followed by a steaming process at 160 °C for 30 min. All treated specimens were placed in the pre-heated autoclave and pressurized steam was applied and regulated to the corresponding prescribed temperature. The treated specimens were then cooled down to room temperature inside the autoclave and then conditioned to an equilibrium moisture content (EMC) of approximately 12%, by storing in a constant environment room maintained at a constant 20 °C, 65% relative humidity (RH) for at least 20 days. For comparison, specimens were high-temperature steam treated in the autoclave for 30 min at 160 °C as described in a previous study (Yin et al., 2011).

Small wood pieces containing an integrated growth ring were prepared from the surface of the treated samples (Fig. 1A) and then divided into five pieces (Fig. 1B). The specimens represented wood from approximately annual rings of an age of 30 years. One piece was use to slice transverse sections of 20 μm thickness for imaging FT-IR measurement. Three pieces were used for preparation of micro-specimen of the dimensions (10 × 10 × 1 mm) for moisture sorption testing. Each of them represented a dry mass of approximately 50 mg. One piece was divided into approximately 2 mm long sticks and embedded after freeze drying into Spurr epoxy resin for nanoindentation testing. Similarly, specimens of native spruce wood were prepared as reference materials.

2.2. Microscopic observations

Embedded wood samples were polished across the tracheids using a fine grinder to prepare the surfaces so that their quality would be suitable for microstructure observations under a stereomicroscope before nanoindentation measurement.

2.3. Imaging Fourier transform infrared spectroscopy (FT-IR) microscopy

Chemical changes in the secondary cell wall of tracheids were characterized by imaging FT-IR microscopy in the mid-IR range. The transmission mode was applied on a Spectrum Spotlight 400 imaging FT-IR system (Perkin Elmer Inc., Shelton, CT, USA). From each specimen, three areas of 150 by 150 μm were randomly selected in the earlywood and latewood of a transverse section (Fig. 2A), respectively, using a visible CCD camera. Using a specially designed array detector, scanning was carried out on 16 elements, providing a resolution of 6.25 × 6.25 μm. Eight scans per pixel were added to improve the signal-to-noise ratio (*S*/*N*). The spectra were recorded with 4 cm^{-1} spectral resolution between 4000 cm^{-1} and 720 cm^{-1} and a total full-spectral image (Fig. 2B) of each selected region was then obtained.

The obtained IR spectra were then processed by the software Spotlight 1.5.1, Hyperview 3.2 and Spectrum 6.2.0 developed by Perkin Elmer Inc. The functions of atmosphere correction, flat correction and baseline offset correction were applied in turn to create corrected spectra. Base-line correction was applied at 1800, 1548, 840 and 780 cm^{-1}. Ten pixel positions corresponding to the secondary cell wall in each of the scanning areas were randomly selected for assessing average spectra of each specific area. The spectra were normalized to 1.0 at the cellulose 1425 cm^{-1} peak in order to compare the relative composition in different samples. By focusing on the secondary wall of transverse wood sections the eventual influence on the spectra from redistributed extractives, due to the heat treatment (Yin et al., 2011), was minimized.

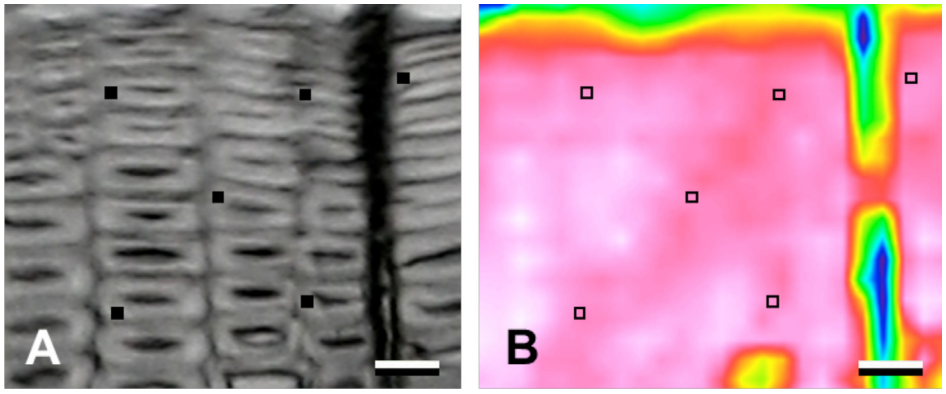

Fig. 2. Visible-light microscopy images of untreated latewood (A). Corrected total full-spectral IR absorbance images of untreated latewood (B). The small black empty box indicates typical pixel position corresponding to the position of the secondary cell wall (black solid box) for measurement of cell wall spectra. Scale bar = 20 μm.

2.4. Moisture sorption

The moisture sorption characteristics were determined on micro-specimens of 50 mg in the range of RH between 0% and 95% at 32 °C using a dynamic vapour sorption (DVS) system (DVS-1085, Surface Measurement System Ltd., UK). The weight changes of the earlywood and latewood sample were determined, respectively, by an electronic microbalance with an accuracy of 0.1 μg. At each RH equilibrium was assumed at a weight change of less than 0.2 μg. The mass change was related to the dry weight of the sample.

2.5. Nanoindentation measurement

The embedded wood samples were polished and then adopted for nanoindentation detection after microscopic observation. The nanoindenter (Hysitron TI700-Ubi, USA) was set up to create images (Fig. 3A and B) and then perform axial indentations on the transverse cell wall surfaces of earlywood and latewood sections. The tip of a diamond Berkovich three-sided pyramid, with a force resolution of ca. 50 nN and a displacement resolution of about 0.1 nm was used to image, locate and indent the secondary cell wall of earlywood and latewood tracheids. A loading function was applied to load a peak force of 250 μN at a loading rate of 100 μN/s, hold at constant load for 15 s and unload at a rate of 100 μN/s (Gindl et al., 2004). The quasi-static mode was used to monitor and record the load, P, and the displacement, h, of the indenter. The so called reduced elastic modulus (E_s) was deduced from the load-displacement data of the retracting force part, $S = dP/dh$, according to Eq. (1) (Gindl et al., 2004). The hardness, H, was determined from the peak load, P_{max}, and the contact area, A, based on the Oliver–Pharr method (Oliver & Pharr, 1992), $H = P_{max}/A$. The elastic modulus of the secondary cell wall in its longitudinal direction was then calculated using Eq. (2), where E is the elastic modulus and v is Poisson ratio for the wood sample and for the indenter, respectively.

$$E_s = \frac{1}{2 \times 1.034}\sqrt{\pi}\frac{S}{\sqrt{A}} \quad (1)$$

$$\frac{1}{E_s} = \frac{1 - v_{wood}^2}{E_{wood}} + \frac{1 - v_{indenter}^2}{E_{indenter}} \quad (2)$$

The diamond indenter has an elastic modulus of 1140 GPa and Poisson ratio of 0.07 (Oliver & Pharr, 1992). Due to the large difference in stiffness between the indenter and the wood material the difference between E_s and E_{wood} may be considered negligible (Gindl et al., 2004). Here, E_s was used as identical to E_{wood} for the evaluation of elastic modulus properties of the secondary cell wall.

Only the indents placed at valid positions, i.e. clearly on secondary cell walls, were used for the final analysis (Fig. 3C and D). An average value from at least 25 indentations, measured in different cell walls, was used for the average properties for each different condition.

3. Results and discussion

3.1. Microscopic observations

For the untreated sample, the typical different features in cell structure between natural earlywood and latewood were clearly observed within a growth ring (Fig. 4A). This also resulted in significantly different deformations of the morphological structure of tracheids and ray cells between earlywood and latewood under

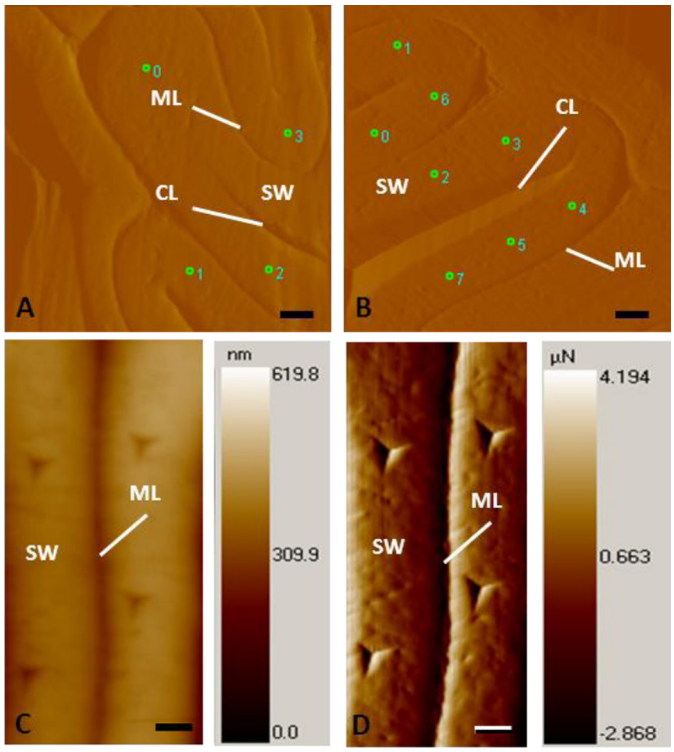

Fig. 3. AFM Images of indents created on the CS-treated earlywood (A) and latewood (B). The number indicates the setting location of indent on the sample surface. AFM image on height mode (C) and load mode (D) of indents created on the secondary cell wall of the earlywood tracheids. Scale bar = 2 μm; SW, the secondary cell wall; ML, middle lamella; CL, cell lumen.

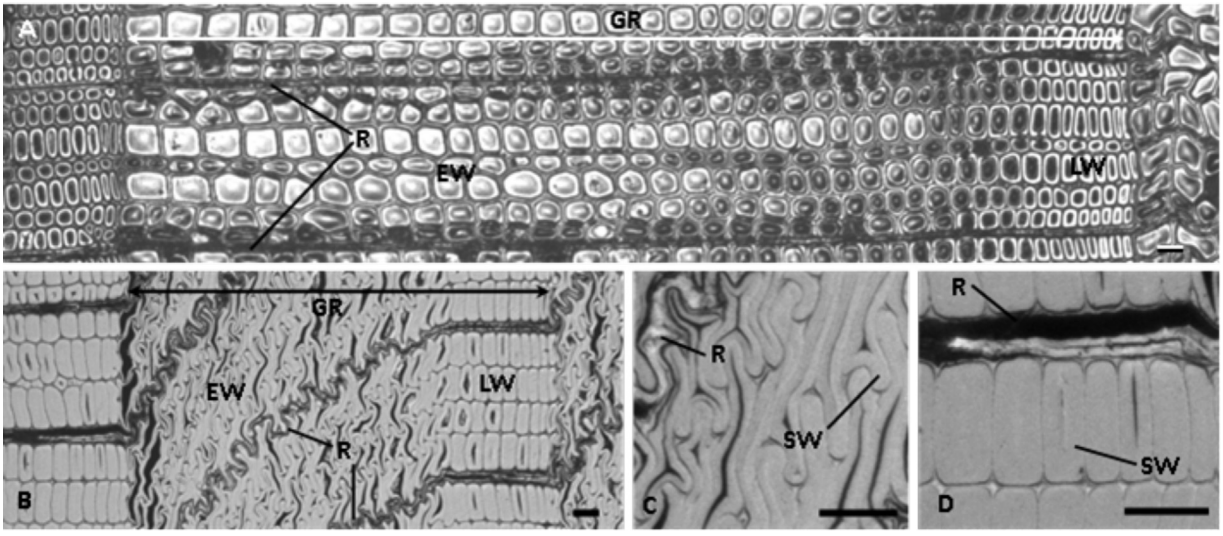

Fig. 4. Visible-light microscopy of cross-section of Spruce wood without treatment, (A); CS-treatment, (B); magnifications of (B) graph, earlywood (C) and latewood (D) sections. GR, growth ring; R: ray; EW: early wood; LW: late wood; SW, the secondary cell wall. Scale bar = 20 μm.

CS-treatment (Fig. 4B). Cell lumens of all tracheids in both the earlywood and latewood regions were almost closed. Much greater distortion of the cell wall occurred in tracheids and rays of earlywood (Fig. 4C) and less deformation of the cell wall was found in latewood (Fig. 4D). The rays of earlywood were deformed into a "zigzag" shape (Fig. 4B and C), whereas no such shape was observed in the latewood.

The tracheids in earlywood almost collapsed, whilst this was not observed in latewood, in accordance with previous studies (Kunesh, 1968; Bodig, 1965; Schrepfer & Schweingruber, 1998). In general, cells of earlywood possess larger lumen with thin and a less-dense cell wall than latewood. Since the radial compression treatment was carried out at a temperature of 160 °C, which was higher than the glass transition temperatures of both hemicellulose and lignin (Hillis & Rozsa, 1978, 1985; Murugan, Mahinpey, Johnson, & Wilson, 2008), the enhanced mobility of hemicellulose and lignin molecules within and between the fibres, leads to a more deformed structure. Due to the high deformation of the earlywood cell walls probably additional pores in different sizes (mesopore or micropore) were formed in these thin-wall cells of earlywood. For the less distorted latewood, a slight densification of the cell wall might arise. Subsequently, the changes in configuration of tracheid and ray cells of earlywood and latewood were then permanently fixed by the further steam process following the compression treatment.

3.2. Imaging FT-IR spectra of the cell wall

The chemical structure of the wood polymers in the cell wall is a very important factor for an in-depth understanding of the physical and mechanical performance of wood cell walls. The hemicelluloses (xylan and glucomannan) play an essential role, by acting as a bonding agent between cellulose and lignin in the construction of the cell wall.

Compared with the native wood sample, chemical changes were observed after CS-treatment for both earlywood (Fig. 5A) and latewood (Fig. 5C). For cellulose the 1316 cm^{-1} and 1336 cm^{-1} bands ascribed to CH_2 wagging vibrations in the crystalline cellulose and to OH in plane bending of amorphous cellulose, respectively (Colom et al., 2003; Huang et al., 2013; Lionetto et al., 2012), may be used to assess structural changes in cellulose. Thus the absorbance ratio of I_{1316}/I_{1336} provides additional information concerning the difference in the degradation process of amorphous and crystalline cellulose (Huang et al., 2013) where an increase in the ratio indicates an increase in the relative crystalline cellulose content (Lionetto et al., 2012). The ratio I_{1316}/I_{1336} remained almost constant in all samples except for CS treated samples where an increase was found for both earlywood and latewood (Table 1). This indicates that an increase in the relative crystalline cellulose content became significant only if wood was compressed under steam treatment.

For hemicellulose and lignin, the characteristic peaks at 1738 cm^{-1}, 1596 cm^{-1}, and 810 cm^{-1}, belonging to C=O stretching vibrations in the O=C—OH group of glucuronic acid unit in xylan (Stevanic & Salmén, 2009; Liang et al., 1960; Marchessault, 1962; Åkerholm & Salmén, 2001), to the aromatic skeletal vibrations plus C=O stretch of lignin (Faix, 1991; Åkerholm & Salmén, 2003), and to vibrations caused by the equatorially aligned hydrogen at the C_2 atom in the mannose residue of glucomannan, (Stevanic & Salmén, 2009; Liang et al., 1960; Marchessault, 1962; Åkerholm & Salmén, 2001), respectively, clear changes for both earlywood (Fig. 5B) and latewood (Fig. 5D) were observed. In general, the relative intensities of the absorption peaks at 1738 cm^{-1}, 1596 cm^{-1} and 810 cm^{-1} for both earlywood and latewood decreased (Fig. 5B and D) under CS-treatment, indicating that the treatment led to degradation of C=O in the O=C—OH group of the glucuronic acid unit of xylan, a loss of the C=O group linked to the aromatic skeleton in lignin, as well as a decomposition of the glucomannan backbone. A clear difference was observed between the behaviour of earlywood and latewood for CS-treatment, in comparison with those after pure steam treatment (Yin et al., 2011).

The relative intensities of the xylan band at 1738 cm^{-1} and the glucomannan band at 810 cm^{-1} both decreased compared to native wood samples after CS-treatment (Fig. 5B and D). On the contrary, the xylan band at 1456 cm^{-1} ascribed to CH_2 symmetric bending on the xylose ring (Stevanic & Salmén, 2009; Liang et al., 1960; Marchessault, 1962; Åkerholm & Salmén, 2001) and the peak at 1236 cm^{-1} belonging to the C—O stretching in the O=C—O group (Stevanic & Salmén, 2009; Liang et al., 1960; Marchessault, 1962; Åkerholm & Salmén, 2001), only showed small changes for both ealywood and latewood; for 1456 cm^{-1} (<4.0% for earlywood and <0.5% for latewood) and for 1236 cm^{-1} (<9.9% for earlywood and <3.2% for latewood). As the 1456 cm^{-1} peak, associated to the xylan backbone, was nearly unaffected it is probable that no major degradation of the xylan backbone had occurred, and that the primary effect on the xylan was a side group splitting (Dwianto et al., 2005; Dietrichs et al., 1978; Boonstra et al., 1998; Garrote et al., 2001).

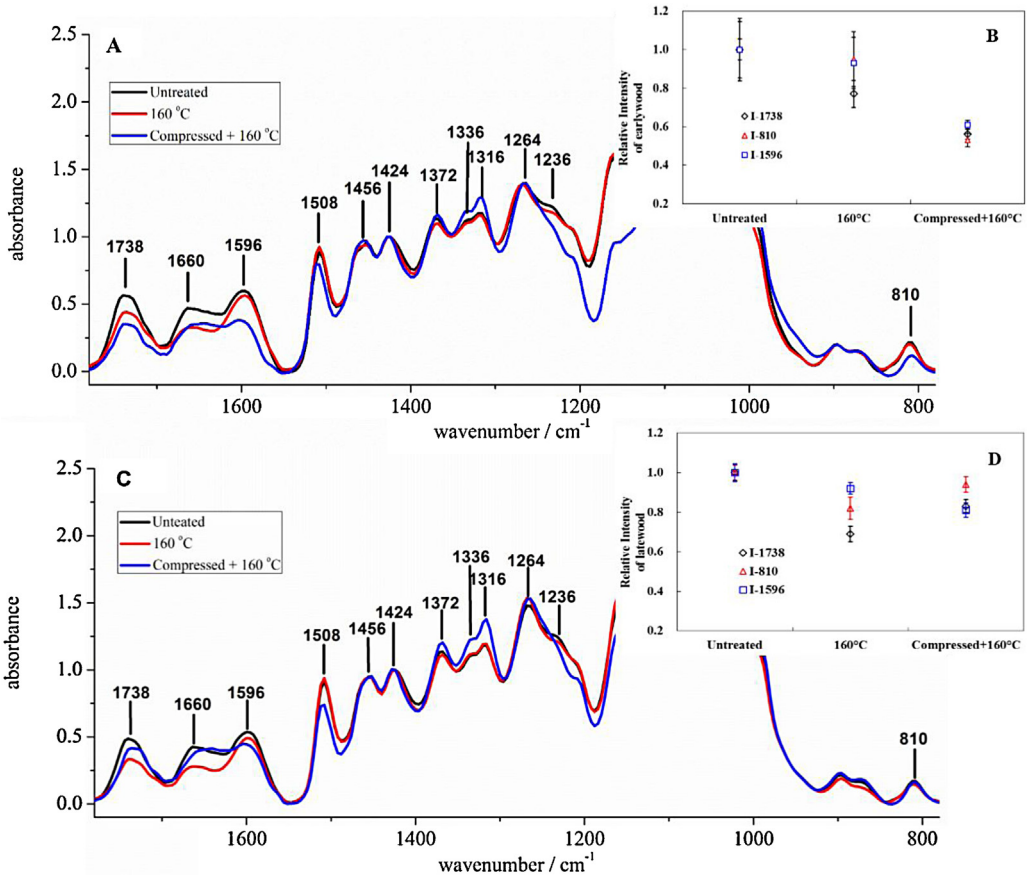

Fig. 5. FT-IR spectra of the secondary cell wall of earlywood (A) and latewood (C) in the fingerprint region. Black line: samples without treatment; red line: samples with steam treatment at 160 °C; blue line: samples with CS-treatment. The relative intensities of the absorption peaks at 1738, 1596, and 810 cm^{-1} in earlywood (B) or latewood (D) as a function of treatments. (For interpretation of the references to color in this figure legend, the reader is referred to the web version of this article.)

Table 1
Absorbance ratios of wood samples.

Sample	I_{1316}/I_{1336} for earlywood	I_{1316}/I_{1336} for latewood
Native wood	1.054	1.070
Steam treated wood	1.057	1.069
CS treated wood	1.094	1.127

Compared with the wood that only had been steam treated, both xylan and glucomannan displayed greater degradation for earlywood and less degradation for latewood under CS-treatment. Specifically, for the C=O in the O=C–OH group of the glucuronic acid unit of xylan at 1738 cm^{-1} and the glucomannan band at 810 cm^{-1} the relative intensities in earywood decreased 44% and 47%, respectively. These chemical changes might be related to the effect of the compression which presumably created more porous structures in earlywood due to the heavy distortion of the cell wall but caused a closure of lumens in latewood. Such pores, small cracks, and more open lumens would facilitate penetration of steam, leading to higher degradation of hemicellulose structures in the earlywood.

Also for lignin, band 1596 cm^{-1} showed a larger decrease; 39% for earlywood and 19% for latewood after CS-treatment (Fig. 5B and D). The intensity changes were though not as large for other absorption bands, 1508 cm^{-1} (Bodig, 1965; Hillis & Rozsa, 1978, 1985) and 1264 cm^{-1} (Hillis & Rozsa, 1978, 1985) ascribed to the aromatic skeletal vibration and the vibration of the guaiacyl ring, together with the C=O stretch, respectively; 1508 cm^{-1} (<10.1% for earlywood and <19.5% for latewood) and 1264 cm^{-1} (<0.1% for earlywood and <3.9% for latewood) after CS-treatment. The larger changes in the relative intensity at 1596 cm^{-1}, in combination with the lower change in intensity at 1508 cm^{-1}, indicate that a loss of the C=O group linked to the aromatic skeleton of lignin has probably occurred. This could indicate that cross-links have been formed between aromatic units in the lignin.

Obviously different behaviours are noted for hemicelluloses and lignin in respect to the degradation under pure steam conditions and that under CS-treatment for earlywood and latewood. This points to that the degradation of hemicelluloses and lignin follows different path ways. Lignin cross-linking is probably a radical reaction (Bardet et al., 1985; Ramos, 2003) which might be favoured by the increased density of the wood material while the hemicellulose degradation is probably more favoured by the more open access to dissolution of carbohydrates (Garrote et al., 2001; Ramos, 2003).

3.3. Moisture sorption isotherms

The moisture sorption isotherms for the native, steam treated, and CS treated earlywood and latewood samples are shown in Fig. 6. After the CS-treatment, clear decreases in moisture uptake were observed for both earlywood and latewood, compared with that in native wood samples; the moisture content (MC) in absorption was 12% and 13% lower in average than that obtained from native wood for earlywood (Fig. 6C) and latewood (Fig. 6D), respectively. Also, in the desorption, a lower moisture content was observed for the treated wood.

Hygroscopicity is highly correlated with the accessible hydroxyl groups in wood (Tjeerdsma & Militz, 2005). The reduction in

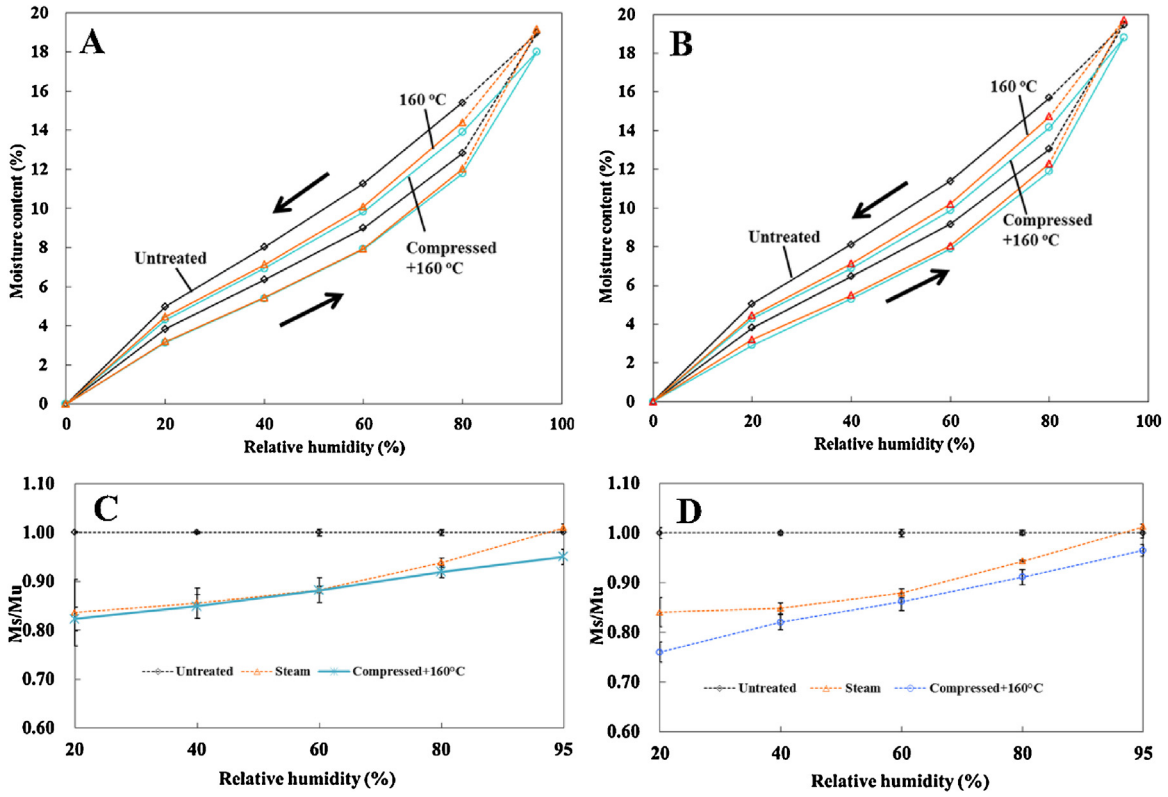

Fig. 6. Sorption isotherms of untreated, steam-treated at 160 °C, and a CS-treated spruce earlywood (A) and latewood (B) samples within the relative humidity (RH) interval of 0-95%, respectively. And relative change in equillibrium moisture content (Ms/Mu) in absorption of spruce earlywood (C) and latewood (D) subjected to treatments as function of relative humidity (RH), respectively. Ms = moisture content (MC) of treated specimens; Mu = MC of untreated specimens.

hygroscopicity of the wood after CS-treatment probably reflects a reduction of accessible hydroxyl groups during treatment. As indicated by the imaging FT-IR spectra, the hemicellullose and lignin components were changed after CS-treatment; a degradation of xylan and a loss of glucomannan, as well as a loss of C=O groups linked to the aromatic skeleton in lignin (Fig. 5). Due to the higher degradation of hemicellulose and lignin in cell walls after CS-treatment, as discussed above, the hygroscopticity of wood treated by CS-treatment was less than that of wood only subjected to steam treatment; 9.5% and 10% lower in average than that obtained from native wood for earlywood (Fig. 6C) and latewood (Fig. 6D), respectively. Furthermore, the relative crystalline cellulose content increases after CS-treatment, as discussed above, resulting in a decreased accessibility of hydroxyl groups to water molecules (Wikberg & Maunu, 2004; Bhuiyan & Hirai, 2005; Boonstra & Tjeerdsma, 2006), which also contributes to a reduction in hygroscopicity. Differences in hygroscopic behaviour are not easily linked to the chemical composition of wood. It is however here clear that the large structural changes in lignin during CS-treatment, especially in the case of latewood indicates that lignin probably plays a key role in the hygroscopticity of the cell wall, as reported by Repellin and Guyonnet (2005).

3.4. Mechanical properties of the cell wall

Nanoindentation technique was used to measure the stiffness of the cell wall on a submicrometer level. Furthermore, an atomic force microscope (AFM) attached by the nanoindenter was used to validate the position and quality of indents made in the secondary cell wall. Positions on the edge of the cell wall were consequently disregarded. The average indentation modulus (E) values and hardness values for the secondary cell wall, determined from the nanoindentation and load-displacement data, as shown in Fig. 7, both showed a decreasing trend of the stiffness after steam treatment, but a significant improvement under CS-treatment, both for earlywood and latewood. The wood samples after CS-treatment had the highest indentation modulus of 18.8 and 20.0 GPa and the highest hardness of 0.4 and 0.45 GPa for the secondary cell walls in earlywood and latewood, respectively. Furthermore, the average E and hardness of wood sample after treatments was always higher for latewood than that for earlywood, respectively (Fig. 7B), which is consistent with previous studies (Yin et al., 2011; Mikkola & Korhonen, 2013; Wimmer et al., 1997).

The rigidity of the cell wall probably arises both from the crystallinity of cellulose in the fibrils and from the cross-linking of lignin in the matrix (Jarvis & McCann, 2000). As indicated in previous studies (Todaro et al., 2012; Yin et al., 2011; Ramos, 2003), the change of strength is mainly due to the variations of interactions among wood polymers after treatments. The differences between the effects of a pure steam treatment as compared to the CS-treatment are probably related to differences in the density of the cell wall and the crystallinity of the cellulose in the fibrils. During normal steam treatment the degradation of cell wall components will result in dissolution of material leaving the cell wall more porous in similarity with normal pulping. This will result in a lower density of the cell wall with less support for the cellulose crystalline aggregates and thus lower strength and stiffness. In contrast, during the CS-treatment the mechanical compression may compensate for the creation of pores by a compaction of the cell wall creating support for the crystalline aggregates and a higher density of these aggregates. Moreover, the increase in the relative crystalline cellulose content in the fibrils after CS-treatment also leads to improvement of mechanical properties, i.e. an enhanced strength and stiffness of the wood.

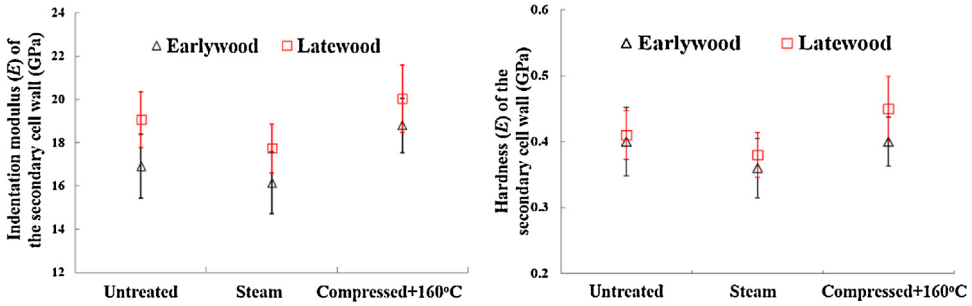

Fig. 7. (A) Indentation modulus (E), determined by nanoindentation, of the secondary cell wall of earlywood and latewood as a function of treament processes. (B) Hardness, determined by nanoindentation, of the secondary cell wall of earlywood and latewood as a function of treatment processes.

4. Conclusion

The procedure of compression combined with steam treatment (CS-treatment) applied in this investigation caused clear changes in morphological, chemical, mechanical and hygroscopical properties of the secondary cell wall. Compared with pure steam treatment, the compression involved in CS-treatment probably creates pores and cracks in cell wall due to the distortion of the cell wall. Such pores and small cracks could facilitate penetration of steam, leading to higher degradation of hemicelluloses, lignin and of amorphous cellulose leading to a higher relative crystalline cellulose content in the fibrils. Imaging (FT-IR) microscopy indicated a progressive degradation of C═O in the O═C—OH group of the glucuronic acid unit of xylan, a decomposition of the glucomannan backbone, and a loss of C═O groups linked to the aromatic skeleton in lignin. Furthermore, the relative crystalline cellulose content in the fibrils increased after CS-treatment. These changes decreased the accessible moisture sorbing sites in the wood, resulting in a lower hygroscopicity. In contrast to cell walls under pure steam treatment, the degradation of the biopolymer components in the secondary cell wall was larger under CS-treatment. However, the applied compression forces resulted in a stiffer and stronger structure probably as a result of the higher cell wall density. Also the higher relative crystalline cellulose content in the fibrils gives the cellulose aggregate structure a higher stiffness resulting in a better support of these load bearing structures.

Author contributions

The manuscript was written through contributions of all authors. All authors have given approval to the final version of the manuscript.

Acknowledgements

This study was sponsored by the Wallenberg Wood Science Center (WWSC) of the Royal Institute of Technology (KTH) of Sweden. Yafang Yin gratefully acknowledges financial support by the Chinese National Natural Science Foundation (no. 31370559) and the China Scholarship Council (CSC), and the approval of a short term scientific mission (STSM) by the COST (European Cooperation in the field of Scientific and Technical Research) Action FP0802 for financial support of a visit to Max-Planck Institute of Colloids and Interfaces for nanoindentation testing. The technical help from Professor Lars Berglund of KTH for the discussion of experimental design, Dr. Toshiro Morooka of Research Institute for Sustainable Humanosphere, Kyoto University, Japan for the compression combined with steam treatment, Anna Jensen of Innventia AB for the steam treatment, Ingela Bjurhager of KTH for micro-sample cutting, Anni Hagberg of Innventia AB for sample embedding, and Dr. Ingo Burgert and Mr. Bo Zhang of the Department of Biomaterials of Max-Planck Institute of Colloids and Interfaces at Potsdam, Germany for instructions of nanoindentation measurement is gratefully acknowledged.

References

Åkerholm, M., & Salmén, L. (2001). Interactions between wood polymers studied by dynamic FT-IR spectroscopy. *Polymer*, *42*, 963–969.
Åkerholm, M., & Salmén, L. (2003). The mechanical role of lignin in the cell wall of spruce tracheids. *Holzforschung*, *57*, 459–465.
Bardet, M., Robert, D. R., & Lundquist, K. (1985). On the reactions and degradation of the lignin during steam hydrolysis of aspen wood. *Svensk Papperstidning*, *6*, 61–67.
Bhuiyan, T. R., & Hirai, N. (2005). Study of crystalline behaviour of heat-treated wood cellulose during treatments in water. *Journal of Wood Science*, *51*, 42–47.
Bodig, J. (1965). The effect of anatomy on the initial stress–strain relationship in transverse compression. *Forest Products Journal*, *15*, 197–202.
Boonstra, M. J., Tjeerdsma, B. F., & Groeneveld, H. A. C. (1998). Thermal modification of non-durable wood species. 1. The PLATO technology: Thermal modification of wood. In *Document no. IRG/WP 98-40123*. Stockholm, Sweden: International Research Group on Wood Preservation.
Boonstra, M. J., & Tjeerdsma, B. F. (2006). Chemical analysis of heat treated softwoods. *Holz- als Roh- und Werkstoff*, *64*, 204–211.
Cai, J. B., Yang, X., Cai, L. P., & Sheldon, Q. S. (2013). Impact of the combination of densification and thermal modification on dimensional stability and hardness of Poplar lumber. *Drying Technology*, *31*, 1107–1113.
Colom, X., Carrillo, F., Nogués, F., & Garriga, P. (2003). Structural analysis of photodegraded wood by means of FTIR spectroscopy. *Polymer Degradation and Stability*, *80*, 543–549.
Deka, M., & Saikia, C. N. (2000). Chemical modification of wood with thermosetting resin: Effect on dimensional stability and strength property. *Bioresource Technology*, *73*, 179–181.
Dietrichs, H. H., Sinner, M., & Puls, J. (1978). Potential of steaming hardwoods and straw for feed and food production. *Holzforschung*, *32*, 193–199.
Diouf, P. N., Stevanovic, T., Cloutier, A., Fang, C.-H., Blanchet, P., Koubaa, A., et al. (2011). Effects of thermo-hygro-mechanical densification on the surface characteristics of trembling aspen and hybrid poplar wood veneers. *Applied Surface Science*, *257*, 3558–3564.
Dwianto, W., Morooka, T., Norimoto, M., & Kitajima, T. (2005). Stress relaxation of Sugi (*Cryptomeria japonica* D. Don) wood in radial compression under high temperature steam. *Holzforschung*, *53*, 541–546.
Ermeydan, M. A., Cabane, E., Masic, A., Koetz, J., & Burgert, I. (2012). Flavonoid insertion into cell walls improves wood properties. *ACS Applied Materials & Interfaces*, *4*, 5782–5789.
Ermeydan, M. A., Cabane, E., Gierlinger, N., Koetz, J., & Burgert, I. (2014). Improvement of wood material properties via in situ polymerization of styrene into tosylated cell walls. *RSC Advances*, *4*, 12981–12988.
Esteves, B., & Pereira, H. M. (2009). Wood modification by heat treatment: A review. *Bioresources*, *4*, 370–404.
Faix, O. (1991). Classification of lignins from different botanical origins by FT-IR spectroscopy. *Holzforschung*, *45*, 21–27.
Fengel, D., & Wegener, G. (1984). *Wood: Chemistry, ultrastructure. Reactions*. Berlin and New York: Walter de Gruyter Press.
Garrote, G., Domínguez, H., & Parajó, J. C. (2001). Study on the deacetylation of hemicelluloses during the hydrothermal processing of *Eucalyptus* wood. *Holz- als Roh- und Werkstoff*, *59*, 53–59.
Gershon, A. L., Bruck, H. A., Xu, S. W., Sutton, M. A., & Tiwari, V. (2010). Multiscale mechanical and structural characterizations of Palmetto wood for bio-inspired hierarchically structured polymer composites. *Materials Science and Engineering: C*, *30*, 235–244.
Gindl, W., Gupta, H. S., Schöberl, T., Lichtenegger, H. C., & Fratzl, P. (2004). Mechanical properties of spruce wood cell walls by nanoindentation. *Applied Physics A*, *79*, 2069–2073.

Havimo, M., Rikala, J., Sirviö, J., & Sipi, M. (2007). Distributions of tracheids cross-sectional dimensions in different parts of Norway Spruce stems. *Silva Fennica*, *42*, 89–99.
Hill, C. A. S. (2006). *Wood modification: Chemical, thermal and other processes*. New York, NY: Wiley Press.
Hillis, W. E., & Rozsa, A. N. (1978). The softening temperatures of wood. *Holzforshung*, *32*, 68–73.
Hillis, W. E., & Rozsa, A. N. (1985). High temperature and chemical effects on wood stability. Part 2. The effect of heat on the softening of radiate pine. *Wood Science and Technology*, *19*, 57–66.
Homan, W. J., & Jorissen, A. J. M. (2004). Wood modification developments. *Heron*, *49*, 361–386.
Huang, X. N., Kocaefe, D., Kocaefe, Y., Boluk, Y., & Krause, C. (2013). Structural analysis of heat-treated birch (*Betule papyrifera*) surface during artificial weathering. *Applied Surface Science*, *264*, 117–127.
Inoue, M., Norimoto, M., Otsuka, Y., & Yamada, T. (1990). Surface compression of coniferous wood lumber. I. A new technique to compress the surface layer. *Journal of the Japan Wood Research Society*, *36*, 969–975.
Jarvis, M. C., & McCann, M. C. (2000). Macromolecular biophysics of the plant cell wall: Concepts and methodology. *Plant Physiology and Biochemistry*, *38*, 1–13.
Jebrane, M., & Sèbe, G. (2008). A new process for the esterification of wood by reaction with vinyl esters. *Carbohydrate Polymers*, *72*, 657–663.
Jebrane, M., Pichavant, F., & Gilles, S. (2011). A comparative study on the acetylation of wood by reaction with vinyl acetate and acetic anhydride. *Carbohydrate Polymers*, *83*, 339–345.
Kollmann, F. F. P., Kuenzi, E. W., & Stamm, A. J. (1975). *Principles of wood science and technology: Wood based materials, manufacture and properties*. New York, Heidelberg, Berlin: Springer-Verlag Press.
Kunesh, R. H. (1968). Strength and elastic properties of wood in transverse compression. *Forest Products Journal*, *18*, 65–72.
Kutnar, A., & Šernek, M. (2007). Densification of wood. *Zbornik gozdarstva in lesarstva*, *82*, 53–62.
Lam, P. S., Lam, P. Y., Sokhansanj, S., Bi, X. T., & Lim, C. J. (2013). Mechanical and compositional characteristics of steam-treated Douglas fir (*Pseudotsuga menziesii* L.) during pelletization. *Biomass & Bioenergy*, *56*, 116–126.
Liang, C. Y., Bassett, K. H., McGinnes, E. A., & Marchessault, R. H. (1960). Infrared spectra of crystalline polysaccharides. VII. Thin wood sections. *TAPPI*, *43*, 1017–1024.
Lionetto, F., Sole, R. D., Cannoletta, D., Vasapollo, G., & Maffezzoli, A. (2012). Monitoring wood degradation during weathering by cellulose crystallinity. *Materials*, *5*, 1910–1922.
Marchessault, R. H. (1962). Application of infrared spectroscopy to cellulose and wood polysaccharides. *Pure and Applied Chemistry*, *5*, 107–129.
Mikkola, M. T., & Korhonen, R. K. (2013). Effect of latewood proportion on mechanical properties of Finnish Pine wood modified with compression drying. *Wood and Fiber Science*, *45*, 335–342.
Murugan, P., Mahinpey, N., Johnson, K. E., & Wilson, M. (2008). Kinetics of the pyrolysis of lignin using thermogravimetric and differential scanning calorimetry methods. *Energy Fuels*, *22*, 2720–2724.
Navi, P., & Girardet, F. (2005). Effects of thermo-hydro-mechanical treatment on the structure and properties of wood. *Holzforschung*, *54*, 287–293.
Oliver, W. C., & Pharr, G. M. (1992). An improved technique for determining hardness and elastic modulus using load and displacement sensing indentation experiments. *Journal of Materials Research*, *7*, 1564–1583.
Panshin, A. J., & Zeeuw, C. D. (1970). *Textbook of wood technology: Structure, identification, properties, and uses of the commercial woods of the United States and Canada. McGraw-Hill series in forest resources* (vol. 1) Ontario: McGraw-Hill College Press.
Ramos, L. P. (2003). The chemistry involved in the steam treatment of lignocellulosic materials. *Química Nova*, *26*, 863–871.
Repellin, V., & Guyonnet, R. (2005). Elvaluation of heat treated wood swelling by differential scanning calorimetry in relation to chemical composition. *Holzforschung*, *59*, 28–34.
Richter, H. G., Grosser, D., Heinz, I., & Gasson, P. E. (2004). IAWA list of microscopic features for softwood identification. *IAWA Journal*, *25*, 1–70.
Schrepfer, V., & Schweingruber, F. H. (1998). Anatomical structures in reshaped press-dried wood. *Holzforschung*, *52*, 615–622.
Stevanic, J. S., & Salmén, L. (2009). Orientation of the wood polymers in the cell wall of spruce wood fibres. *Holzforschung*, *63*, 497–503.
Tjeerdsma, B. F., & Militz, H. (2005). Chemical changes in hydrothermal treated wood: FTIR analysis of combined hydrothermal and dry heat-treated wood. *Holz- als Roh- und Werkstoff*, *63*, 102–111.
Todaro, L., Zanuttini, R., Scopa, A., & Moretti, N. (2012). Influence of combined hydrothermal treatments on selected properties of Turkey oak (*Quercus cerris* L.) wood. *Wood Science and Technology*, *46*, 563–578.
Tooyserkani, Z., Sokhansanj, S., Bi, X., Lim, J., Lau, A., Saddler, J., et al. (2013). Steam treatment of four softwood species and bark to produce torrefied wood. *Applied Energy*, *103*, 514–521.
Trey, S. M., Netrval, J., Berglund, L., & Johansson, M. (2010). Electron-beam-initiated polymerization of poly(ethylene glycol)-based wood impregnants. *ACS Applied Materials & Interfaces*, *2*, 3352–3362.
Vincent, M., Tong, Q., Terziev, N., Daniel, G., Bustos, C., Escobar, W. G., et al. (2014). A comparison of nanoindentation cell wall hardness and Brinell wood hardness in jack pine (*Pinus banksiana Lamb.*). *Wood Science and Technology*, *48*, 7–22.
Welzbacher, C. R., Wehsener, J., Rapp, A. O., & Haller, P. (2008). Thermo-mechanical densification combined with thermal modification of Norway spruce (*Picea abies* Karst) in industrial scale-Dimensional stability and durability aspects. *Holz- als Roh- und Werkstoff*, *66*, 39–49.
Wikberg, H., & Maunu, S. L. (2004). Characterisation of thermally modified hard- and softwoods by ^{13}C CPMAS NMR. *Carbohydrate Polymers*, *58*, 461–466.
Wimmer, R., Lucas, B. N., Oliver, W. C., & Tsui, T. Y. (1997). Longitudinal hardness and Young's modulus of spruce tracheid secondary walls using nanoindentation technique. *Wood Science and Technology*, *31*, 131–141.
Yin, Y. F., Berglund, L., & Salmén, L. (2011). Effect of steam treatment on the properties of wood cell walls. *Biomacromolecules*, *12*, 194–202.
Yu, Y., Fei, B. H., Zhang, B., & Yu, X. (2007). Cell-wall mechanical properties of bamboo investigated by in-situ imaging nanoindentation. *Wood and Fiber Science*, *39*, 527–535.
Yuan, T. Q., Zhang, L. M., Xu, F., & Sun, R. C. (2013). Enhanced photostability and thermal stability of wood by benzoylation in an ionic liquid system. *Industrial Crops and Products*, *45*, 36–43.